Simulation study on derivative phase extraction of typical blood cells under interference microscopy

Yuanyuan Xu (徐媛媛)[1], Yawei Wang (王亚伟)[1,2*], Ying Ji (季 颖)[2], and Weifeng Jin (金卫凤)[1]

[1]*School of Mechanical Engineering, Jiangsu University, Zhenjiang 212013, China*
[2]*Faculty of Science, Jiangsu University, Zhenjiang 212013, China*
**Corresponding author: jszjwyw@sina.cn*

Received September 21, 2013; accepted October 15, 2013; posted online February 27, 2014

Quantitative phase imaging (QPI) of biological cells is an important developing technique. In this paper, a derivative method of phase extraction is put out under several typical blood cells' models, which is completed by numerically simulating the process of QPI. Furthermore, the first-order derivative of the phase is introduced to analyze the cell morphology, and a monocyte model is discussed as an example to demonstrate the method. It shows that the first-order derivative of the phase can be used as a tool for the identification of blood cells.

OCIS codes: 100.5070, 180.3170, 170.1530.
doi: 10.3788/COL201412.S11001.

Biological cells are microscopic dynamic objects, and they are capable of continuously adjusting their morphological parameters, such as size, shape, and volume. Related to their various functions and dynamics, these parameters of the cells are important for many researches in biology and life science. However, biological cells are mostly transparent objects, conventional intensity-based light microscopy techniques fail to image them owing to lack of the adequate contrast. Exogenous label contrast agents, such as fluorescence dyes, can solve the contrast problem, but they may make the living cells phototoxic and influence the cellular behavior[1]. Based on this, the label-free visual observation of the cells can be achieved by many optical phase microscopy imaging methods that make use of the optical path delays occurred when light traverses through cells. Traditional methods, such as Zernike phase contrast microscopy[2] and differential interference contrast microscopy[3] are widely used. However, these techniques cannot provide the quantitative information of the cellular structure. Therefore, quantitative phase imaging (QPI) of cells has become an active field of study and various advanced methods have been proposed[4–16], such as digital holography microscopy (DHM)[4–6], Fourier phase microscopy (FPM)[13], spatial light interference microscopy (SLIM)[14], and white light diffraction phase microscopy (wDPM)[15]. QPI is superior to other methods in that it can measure the optical phase shift associated with the cells and offer nanometer scale structure and dynamics information with high speed and without contact. Despite these excellent advantages, the range of QPI applications in biology has been largely limited to the homogeneous objects, such as non-nucleated red blood cells, imaging[17,18]. For inhomogeneous objects, complex optical phase structures, the research of QPI on them is still in the initial stage and meets some challenges in the real optical experiments.

In this paper, typical blood cells, especially inhomogeneous white blood cells, are discussed for the rapid and accurate identification of blood cells. Based on the analysis of their morphological characteristics, the corresponding optical models are built and phase distributions are obtained in the simulation experiments of quantitative phase microscopy imaging. Considering the fast data processing ability of derivative operation and the phase change related to the object, especially for the inhomogeneous object, we apply a derivative method for phase extraction in the case of off-axis interference. In order to determine cell and cellular morphology, the first-order derivative of the phase, called a phase derivative method, is introduced. This work provides a theoretical and technical support for the visual observation and identification of white blood cells.

Blood cells are important components of human blood, which include two main types of cells: erythrocytes and leukocytes. Under normal physiological conditions, these cells have their own morphological structures and the relatively stable numbers. In general, mature erythrocyte lacks nucleus and some organelles with a double-concave disc-shape and the diameter between 7 μm and 8.5 μm. Leukocyte is an approximately spherical and nucleate cell, and it is larger than the erythrocyte in volume. Mature leukocytes can be divided into five types: monocyte, lymphocyte, neutrophil, eosinophil, and basophil. Among them, monocyte, with the diameter between 14 μm and 20 μm, has the largest volume, and its nucleus morophology is various. For lymphocyte, its diameter ranges from 6 μm to 20 μm, and its nucleus shape is an approximately eccentric sphere. Besides, the small lymphocyte, with the diameter between 6 μm and 8 μm, has the largest number in lymphocyte. Neutrophil, eosinophil and basophil, with the diameter between 10 μm and 15 um, are granulocytes. In neutrophil and eosinophil, theirs nucleus is divided into 2 to 5 leaves with similar shape. Basophil has complex and irregular nucleus, which is beyond the study in this work. In this paper, according to the analysis of above cells, we have built a biconcave model for the erythrocyte, a homocentric sphere model for the monocyte, an eccentric sphere mode for

the lymphocyte and a sphere that contains two isometrical ellipsoidal nucleuses for the neutrophil and the eosinophil.

Most QPI techniques employ the principle of interferometry to image transparent biological cells. It is practically important to retrieve quantitative phase information in QPI. So one derivative method is introduced as below.

For an off-axis interference system, the intensity recorded can be given by

$$I(x,y) = I_0(x,y) + \gamma(x,y)\cos[\varphi(x,y) + kx], \tag{1}$$

where $I_0(x,y)$ is a low-frequency function that describes background intensity (a DC component), $\gamma(x,y)$ is the amplitude modulation factor of the interferogram, $\varphi(x,y)$ is the spatial varied phase related to the object, and k is the spatial frequency of fringes. Firstly, when the DC term in Eq. (1) is filtered out, we can obtain the interference term, which is given by

$$I^{(0)} = \gamma\cos[\varphi(x,y) + kx]. \tag{2}$$

Considering that most biological cells are transparent phase objects, both the background intensity I_0 and the amplitude modulation factor $\gamma(x,y)$ are approximately constant over the interferogram, and the phase, φ, caused by the thickness of the object and the refractive index difference between it and the surrounding medium, is a slowly varying function, and thus we can make the following approximation:

$$\frac{\partial I_0}{\partial x} \approx 0, \frac{\partial \gamma}{\partial x} \approx 0, \frac{\partial^2 \varphi}{\partial x^2} \approx 0. \tag{3}$$

This approximation of the phase is easily satisfied, even for some complex-structured phase objects, and it is verified in Ref. [19]. Different to the approximation of the derivative method from Popescu[20], we consider the sensitive phase change between adjacent neighborhoods, which is essential especially for the inhomogeneous object owing to the varied refractive index.

Thus, according to Eq. (3), the transverse first- and second-order derivatives of Eq. (1) can be expressed as

$$I^{(1)} = \frac{\partial I(x,y)}{\partial x} = -\gamma\beta\sin[\varphi(x,y) + kx], \tag{4}$$

$$I^{(2)} = \frac{\partial^2 I(x,y)}{\partial x^2} = -\gamma\beta^2\cos[\varphi(x,y) + kx]. \tag{5}$$

Here,

$$(x,y) = \frac{\partial\ (x,y)}{\partial} + k. \tag{6}$$

Based on Eqs. (2), (4), and (5), the phase distribution induced by the object can be calculated and is given by

$$\varphi(x,y) = \begin{cases} \tan^{-1}\left\{\left[-\dfrac{[I^{(1)}]^2}{I^{(2)}\cdot I^{(0)}}\right]^{1/2}\right\} - kx\left(I^{(1)}\cdot I^{(2)} \geq 0\right) \\ \tan^{-1}\left\{-\left[-\dfrac{[I^{(1)}]^2}{I^{(2)}\cdot I^{(0)}}\right]^{1/2}\right\} - kx\left(I^{(1)}\cdot I^{(2)} < 0\right). \end{cases} \tag{7}$$

According to the above theory, we first image the simulated red blood cell (RBC). Due to the absence of the nucleus and organelles, a RBC can be seen as a homogenous phase object. Therefore, the refractive index of RBC, n_{cell}, is uniform, which can be set as a constant, $n_{\text{cell}} = 1.4$ in our simulation and the refractive index of the cell medium, n_{medium}, is 1.34. Through the simulation, we obtain the phase distribution, which is presented in Fig. 1(a). In addition, for the homogenous object, according to the linear relationship between the phase and the thickness, the thickness distribution can be directly computed from the known phase map, as shown in Fig. 1(b). It clearly shows the special double concave shape of a RBC. Fig. 1(c) shows the horizontal and vertical thickness profiles, which are similar to the experiment results from Popescu obtained by Hilbert phase microscopy[12]. It demonstrates the applicability of the above derivative method of interference microscopy and the correctness of simulation.

Next, we apply the same method to analyze white blood cells (WBCs). Owing to morphological diversity of WBCs, we select four typical types of WBCs mentioned previously as the simulated samples. In our simulations, the refractive indices of the cell nucleus, surrounding plasma and surrounding medium are set to be 1.44, 1.3508 and 1.3408, and are labeled as n_2, n_1 and n_0, respectively. Via the numerical simulations, four typical types of WBCs phase distributions are extracted, as shown in Fig. 2. Figs. 2(a) and (b) are the results of the monocyte and lymphocyte, respectively. Fig. 2(c) is the result of the neutrophil or the eosinophil. Through the analysis, we can obtain some important conclusions: different cell models and different nuclear morphology correspond to different phase maps, and the number of cell nuclei is same as the number of the peak of phase distribution.

Unfortunately, white blood cells are inhomogeneous objects, the phase images cannot be directly translated

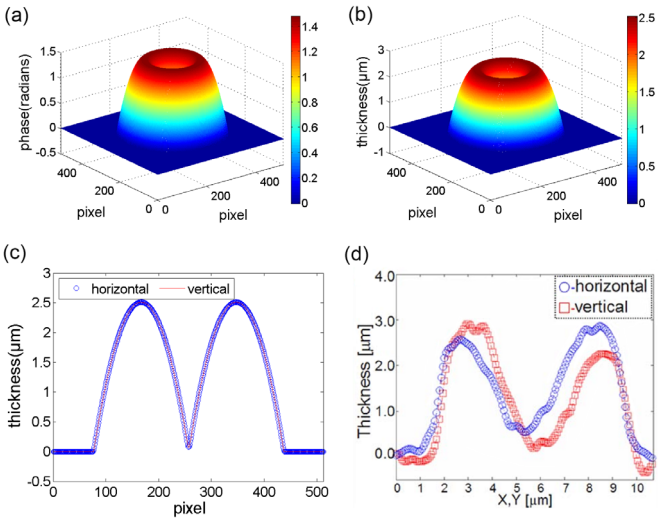

Fig. 1. The red blood cell. (a) The reconstructed phase, the color bar shows the phase in radians, (b) the thickness distribution, the color bar shows the thickness in μm, (c) the horizontal and vertical thickness profiles, and (d) experiment results of thickness[12].

into height maps, which can reveal morphology and dynamic activities of the cell. In fact, it is a common problem for inhomogeneous objects in quantitative phase imaging. The key is to determine the boundary between different mediums with image processing. Here, we introduce a derivative method of phase to analyze cell and nucleus morphology. Via the numerical calculations, the first-order derivatives of phase distributions of four types of WBCs are obtained, which are presented in Fig. 3, in which the morphology and size of cell and nucleus are displayed clearly. These results prove that the first-order derivative of phase is a sensitive parameter to the edges and index-changes in the sample[3,21,22].

In order to further study the phase derivative, we take the monocyte with the concentric sphere model as an example to analyze it. Fig. 4(a) shows the 2D model of the monocyte. Among them n_2, n_1 and n_0 are the refractive indices of the cell nucleus, cytoplasm and surrounding medium respectively, and the relation of $n_2 > n_1 > n_0$ is satisfied. In fact, the phase distribution is an integration of the optical path reduced by the refractive index and the thickness of the sample. So we can infer that the phase derivative is closely related to the change of refractive index. Based on this, the horizontal profile of the phase derivative is done, as shown in Fig. 4(b). There are two larger and two smaller fluctuations, and both have a positive and a negative change, which are symmetrical. Detailed explanation is as follows.

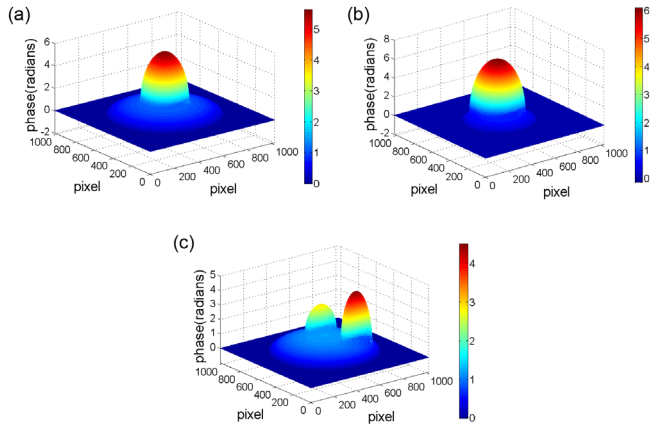

Fig. 2. The phase distributions of typical white blood cells. (a) Monocyte, (b) lymphocyte, and (c) neutrophil or eosinophil.

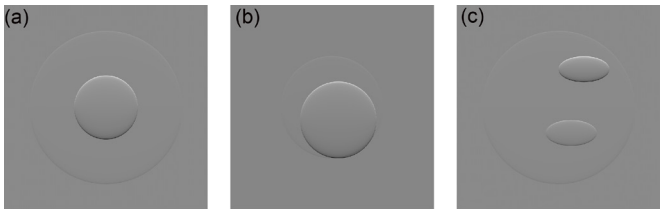

Fig. 3. The phase derivative distributions of typical white blood cells. (a) monocyte, (b) lymphocyte, and (c) neutrophil or eosinophil.

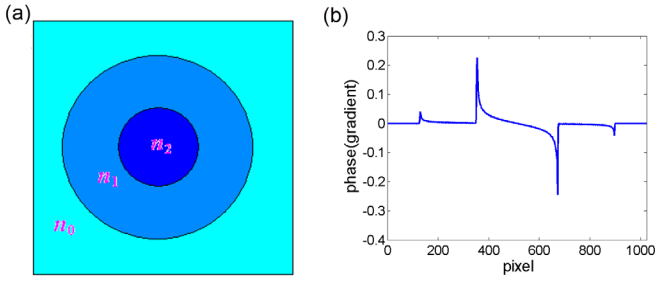

Fig. 4. The monocyte. (a) 2D model and (b) the phase derivative profile.

We assume the light propagates along z-axis. For the horizontal central section of the cell, light goes successively through the surrounding medium, cytoplasm and cell nucleus, and then again passes through cytoplasm and surrounding medium, and therefore the refractive index makes such a change, namely, from n_0 up to n_1, and again up to n_2, and then back to n_1, and last back to n_0. The variation of the phase depends on the change of refractive index when the cell is divided into numerous smaller objects with the identical physical thickness along z-axis. In addition, the change and the derivative operation are based on the concept of the forward difference in the process of numerical calculation. So, there are two positive jumps and two negative jumps for the change of refractive index of the cell, and the positive increment is same as the negative increment. These results are consistent with four fluctuations of Fig. 4(b). Besides, there is a positive correlation between the amplitude of the fluctuation and the increment of refractive index.

In this paper, the quantitative phase images of several typical types of blood cells, especially white blood cells, has been obtained and discussed through numerical simulations. Results has shown that the phase distributions of these cells are closely related to their morphological structures. The phase derivative method is introduced for analyzing cell morphology. It suggests that the derivative of the phase is sensitive to edges and changes of samples by analyzing phase derivative maps of these cells. We believe that this work would provide some reference for the analysis of blood cells in a noninvasive manner.

This work was supported by National Natural Science Foundation of China (NO. 11374130, NO. 11302086), Doctoral Program Joint Fund of colleges and universities Specialized Research (NO. 20113227110018), Jiangsu Province colleges and universities Major Project (NO. 09KJA140001).

References

1. L. J. Kricka and P. Fortina, Clin. Chem. **55,** 670 (2009).
2. F. Zernike, Science **121,** 345(1955).
3. M. G. Nomarski and J. Phys. (Paris) **16,** S9 (1955).
4. E. Cuche, F. Bevilacqua, and C. Depeursinge, Opt. Lett. **24,** 291 (1999).
5. B. Kemper, A.Vollmer, C. E. Rommel, J. Schnekenburger, and G.V.Bally, J. Biomed. Opt. **16,** 026014 (2011).
6. P. Langehanenberg, B. Kemper, D. Dirksen, and G. V. Bally, Appl. Opt. **47,** D176 (2008).
7. N. T. Shaked, M. T. Rinehart, and A. Wax, Opt. Lett. **34,** 767 (2009).

8. N. T. Shaked, Y. Z. Zhu, M. T. Rinehart, and A. Wax, Opt. Express **17,** 15585 (2009).
9. D. Paganin and K. A. Nugent, Phys. Rev. Lett. **80,** 2586 (1998).
10. W. S. Rockward, A. L. Thomas, B. Zhao, and C. A. Dimarzio, Appl. Opt. **47,** 1684 (2008).
11. G. Popescu, T. Ikeda, R. R. Dasari, and M. S. Feld, Opt. Lett. **31,** 775 (2006).
12. G. Popescu, T. Ikeda, C. A. Best, K. Badizadegan, R. R. Dasari, and M. S. Feld, J. Biomed. Opt. **10,** 060503 (2005).
13. G. Popescu, L. P. Deflores, J. C. Vaughan, K. Badizadegan, H. Iwai, R. R. Dasari, and M. S. Feld, Opt. Lett. **29,** 2503 (2004).
14. Z.Wang, L. Millet, M. Mir, H. F. Ding, S. Unarunotai, J. Rogers, M. U. Gillette, and G. Popescu, Opt. Express **19,** 1016 (2011).
15. B. Bhaduri, H. Pham, M. Mir, and G. Popescu, Opt. Lett. **37,** 1094 (2012).
16. B. Bhaduri, K.Tangella, and G. Popescu, Biomed. Opt. Express **4,** 1434 (2013).
17. Y. K. Park, M. Diez-Silva, G. Popescu, G. Lykotrafitis, W. Choi, M. S. Feld, and S. Suresh, Proc. Natl. Acad. Sci. **105,** 13730 (2008).
18. Y. K. Park, C. A. Best, K. Badizadegan, R. R. Dasari, M. S. Feld, T. Kuriabova, M. L. Henle, A. J. Levine, and G. Popescu, Proc. Nat. Acad. Sci. **107,** 6731 (2010).
19. Y. Y. Xu, Y. W. Wang, W. F. Jin, C. H. Lü, and H. Wu, Opt. Commun. **305,** 13 (2013).
20. B. Bhaduri and G. Popescu, Opt. Lett. **37,** 1868(2012).
21. T. Kim, S. Sridharan, and G. Popescu, Opt. Express **20,** 6737 (2012).
22. T. Kim, S. Sridharan, A. Kajdacsy-Balla, K. Tangella, and G. Popescu, Appl. Opt. **52,** A92 (2013).